NÖHÜ Müh. Bilim. Derg. / NOHU J. Eng. Sci., 2025; 14(3), 846-854

Niğde Ömer Halisdemir Üniversitesi Mühendislik Bilimleri Dergisi
Niğde Ömer Halisdemir University Journal of Engineering Sciences

Araştırma makalesi / Research article

www.dergipark.org.tr/tr/pub/ngumuh / www.dergipark.org.tr/en/pub/ngumuh

A practical study of multi-layer high gain U-slot printed antenna array design

Çok katmanlı yüksek kazançlı U-yarık anten dizisi tasarımının pratik bir çalışması

Gülden Günay Bulut Öner[1,*], Asena Melike Çayan[2], Suad Başbuğ[3], Yasemin Altuncu[4]

[1,2,3] *Nevşehir Hacı Bektaş Veli University, Electrical and Electronics Engineering Department,50300, Nevşehir, Türkiye*
[4] *Niğde Ömer Halisdemir University, Electrical and Electronics Engineering Department, 51240, Niğde, Türkiye*

Abstract

In this paper, we propose the design of a multi-layer high-gain U-slot printed antenna array consisting of 2x2 elements.The design consists of four layers: The first layer is a ground plane as a single-sided copper clad FR4. The second layer, made from PETG material, is introduced to enhance the bandwidth of the antenna. Microstrip antenna elements and feed lines are etched into the top segment of the third layer. The fourth layer is a directive structure used to increase the gain of the antenna array, which consists of 8x8 64-elements microstrip patches separated by air gap from the main body. This parasitic layer is supported by four rods fixed to the third layer. According to the results, the simulated center frequency of the proposed design is 2.61 GHz. The maximum gain simulated at 2.61 GHz is 12 dBi, and the measured impedance bandwidth is 14.27%. Additionally, in this study, the fabrication and measurements of the presented antenna were carried out to validate the simulation results. Comparisons between the simulation and measurement data show good agreement in the S_{11} parameter and radiation pattern graphs.

Keywords: Antenna array, High gain, Multi-layer, U-slot antenna

Öz

Bu makalede, 2x2 elemanlardan oluşan çok katmanlı yüksek kazançlı U-yarık anten dizisinin tasarımı sunulmaktadır. Tasarım dört katmandan oluşmaktadır: Birinci katman, tek yüzü bakır kaplanmış FR4 malzemesinden oluşan bir toprak düzlemidir. İkinci katman, antenin bant genişliğini artırmak için PETG malzemesinden yapılmıştır. Üçüncü katmanın üst segmentine mikroşerit anten elemanları ve besleme hatları kazınmıştır. Dördüncü katman, anten dizisinin kazancını artırmak için kullanılan yönlendirilmiş bir yapıdır ve bu yapı, ana gövdeden hava boşluğu ile ayrılmış 8x8'lik 64 elemanlı mikroşerit yama elemanlarından oluşmaktadır. Bu parazitik katman, üçüncü katmana sabitlenmiş dört çubukla desteklenmektedir. Sonuçlara göre, önerilen tasarımın simüle edilmiş merkezi frekansı 2.61 GHz'dir. 2.61 GHz'de simüle edilen maksimum kazanç 12 dBi ve ölçülen empedans bant genişliği %14.27 olarak elde edilmiştir. Ayrıca bu çalışmada, simülasyon sonuçlarının doğrulanması amacıyla sunulan antenin üretimi ve ölçümleri gerçekleştirilmiştir. Simülasyon ve ölçüm verileri arasındaki karşılaştırmalar S_{11} parametresi ve ışıma örüntüsü grafiklerinde iyi bir uyum olduğunu göstermektedir.

Anahtar Kelimeler: Anten dizisi, Yüksek kazanç, Çok katman, U-yarık anten

1 Introduction

High gain, small size and wideband antennas are frequently demanded in the wireless communication applications to improve the data quality and mobility. In this regard, microstrip patch antennas are preferred that they have advantages such as compact size, easy production and low cost compared to the conventional dipole antennas [1]. Microstrip patch antenna is a special type of printed antenna manufactured using methods similar to those used in printed circuits [2]. A conventional microstrip antenna consists of a substrate which has a certain thickness and dielectric constant on a ground plane and a conductive patch on it [3]. Alongside the advantages mentioned above, the microstrip patch antennas have also some disadvantages such as narrow bandwidth and low gain [4]. These disadvantages can be eliminated by design changes made on microstrip patch antennas [5]. Slotted structure used on microstrip patch antennas is one of such design changes [6]. Microstrip patch antennas designed by adding slotted structures have wider bandwidth by comparison with conventional microstrip patch antennas [7]. Microstrip antenna arrays generally consist of patch radiator elements on the same printed circuit board. Besides, it is well known that the gain can be improved by using antenna arrays which cannot be achieved with a single antenna element [8]. Antenna parameters such as gain and bandwidth in microstrip arrays can also be improved by modifications on the ground plane [9-12]. In order to improve the radiation properties, microstrip parasitic elements [13, 14], superstrate structures [15, 16], parasitic layer antenna arrays [17-20], and multi-layer antenna designs [21-23] are used. Also, in the antenna literature 3D printed antennas are frequently studied due to their advantages such as ease of

* Sorumlu yazar / Corresponding author, e-posta / e-mail: ggunaybulut@nevsehir.edu.tr. (G. G. Bulut Öner)
Geliş / Received: 20.02.2025 Kabul / Accepted: 15.04.2025 Yayımlanma / Published: 15.07.2025
doi: 10.28948/ngumuh.1643101

production, transportation cost, and alternative design possibilities in antenna manufacturing compared to classical antenna production techniques [24-26]. Many plastic filaments such as Conformal Polylactic Acid (PLA) [27], Polylactic Acid (PLA) [28, 29], Acrylonitrile Butadiene Styrene (ABS) [30, 31] and Polietilen Tereftalat Glikol (PETG) [32] are commonly used in 3D printed antenna technology. A 2x2 multilayer, broadband antenna array design is presented in [33]. In this study, by using partially reflecting surface (PRS) and reactive impedance surface (RIS) structures, the bandwidth of the design is increased, less gain ripple is obtained and design miniaturization is achieved compared to the design obtained by using only RIS structure. A novel multilayer microstrip patch antenna array fed by substrate-integrated waveguide cavities is reported for Ku-band applications [34]. A dual polarized aperture coupled 2x2 antenna array is fabricated and measured in reference [35]. In [36] the design and fabrication of a stacked, circularly polarized 2x2 meta surface antenna array is realized. In the study given in [37], a 2x2 antenna array design with multilayer quasi-AMC superstrate and Fabry-Perot structure is presented.

In this study, a high gain 2x2 elements multi-layer antenna array design is presented. Multi-layer geometry is designed to increase the bandwidth of the antenna array. With the usage of the PETG material, parameters such as gain and bandwidth can be increased compared to standard single-layer microstrip antenna arrays. By using PETG substrate produced with the help of a three-dimensional printer, antenna substrate with the desired infill and thickness can be produced and in this way, basic antenna parameters such as gain and bandwidth of the antenna design can be improved. An 8x8 64 elements of square microstrip patches are used to increase the gain. This design provides advantages such as ease of production, low cost, high gain, narrow beamwidth and compact profile.

2 Antenna design and analysis

2.1 Antenna array evolution process

In this section, we outline the design stages of the final multi-layer 2x2 microstrip antenna array. The evolution begins with a single-layer U-slot microstrip antenna design operating at a frequency of 2.45 GHz. Following the success of the initial design and simulation, we proceed to the second stage, where a multilayer U-slot microstrip antenna design and simulation are conducted. The introduction of a multilayer structure aims to enhance the bandwidth and gain parameters of the previous design. In the third stage, we realize a multilayer 2x2 4-element microstrip antenna design to further improve the existing radiation parameters. Finally, the design process concludes with the addition of a parasitic layer to the 4-elements U-slot microstrip antenna array, resulting in increased gain compared to the previous stage. The design evolution process is illustrated in Figure 1.

While carrying out the antenna design stages, traditional microstrip patch antenna design formulas [38] are used as a starting point and then the necessary size optimizations are carried out. The initial design formulas in question are given in Equation (1).

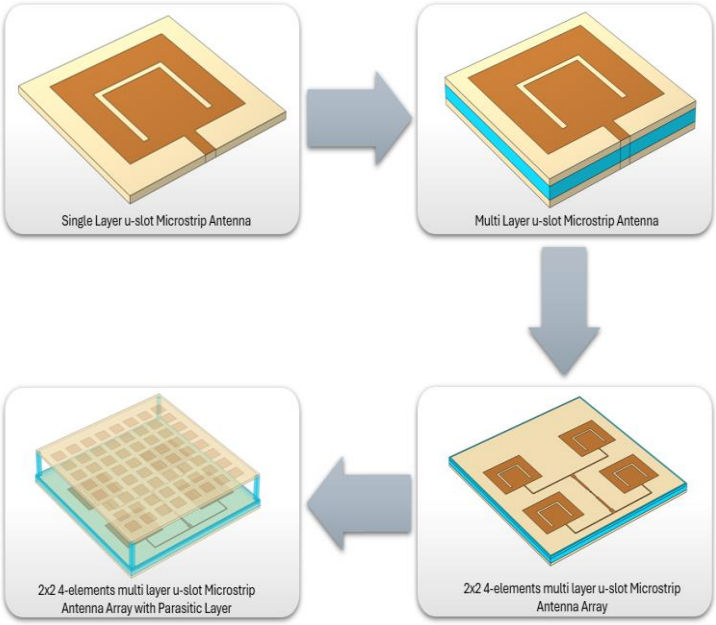

Figure 1. The evolution process of the final antenna array design.

$$\varepsilon_{reff} = \frac{\varepsilon_r + 1}{2} + \frac{\varepsilon_r - 1}{2}\left[1 + 12\frac{h}{W}\right]^{-1/2} \quad (1.a)$$

$$\frac{\Delta L}{h} = 0.412\frac{\left(\varepsilon_{reff} + 0.3\right)\left(\frac{W}{h} + 0.264\right)}{\left(\varepsilon_{reff} - 0.258\right)\left(\frac{W}{h} + 0.8\right)} \quad (1.b)$$

$$L_{eff} = L + 2\Delta L \quad (1.c)$$

$$W = \frac{v_0}{2f_r}\sqrt{\frac{2}{\varepsilon_r + 1}} \quad (1.d)$$

The design parameters for the single-element antenna are depicted in Figure 2, while the optimized values of these parameters for both single-layer and multi-layer antennas are detailed in Table 1. In the single-layer U-slot microstrip antenna design, an FR4 substrate with a dielectric constant (ε_r) of 4.15 and a substrate height (h) of 1.59 mm are chosen due to its several advantages, including low cost and easy fabrication. For the multi-layer U-slot microstrip antenna design, aimed to enhance the antenna parameters such as gain and bandwidth, a sandwich geometry consisting of three layers is utilized. The first and third layers comprise FR4 substrate with a dielectric constant of 4.15 and a substrate height of 1.59 mm. Between these FR4 layers, a layer of Polietilen Tereftalat Glikol (PETG) material is inserted, with a dielectric constant of 2.62 and a thickness (t) of 3 mm.

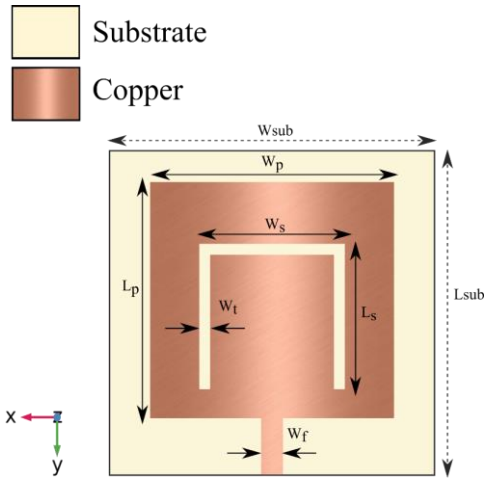

Figure 2. Dimensions of single element U-slot rectangular patch antenna

Table 1. Optimized design parameters of single layer and multi-layer U-slot microstrip antenna

Symbol	Parameter	Value (mm)
Single layer U-slot microstrip patch antenna	Patch Width (W_p)	33.5
	Patch Length (L_p)	32.5
	Slot Width (W_s)	20
	Slot Length (L_s)	20
	Slot Thickness (W_t)	1.5
	Feed Width (W_f)	3
Multi-layer U-slot microstrip patch antenna	Patch Width (W_p)	36
	Patch Length (L_p)	34.58
	Slot Width (W_s)	20
	Slot Length (L_s)	20
	Slot Thickness (W_t)	1.5
	Feed Width (W_f)	3

In order to illustrate the contribution of each design stage, the reflection coefficient plots and realized far field gain plots to the corresponding design stage are presented in Figure 3 and 4, respectively.

When the simulated reflection coefficient plots in Figure 3 are examined, it can be clearly seen that the U-slot microstrip antenna with multi-layer structure exhibits a wider impedance bandwidth (%3.18) compared to the single-layer U-slot microstrip antenna (%1.55). Furthermore, it is observed that the 4-element U-slot microstrip patch antenna array design with a multi-layer structure demonstrates a much wider impedance bandwidth (%12.86) compared to the single-element multi-layer U-slot microstrip patch antenna design. Finally, when the multilayer 2x2 U-slot antenna array is compared with the version with a parasitic layer added to this design, it is observed that the impedance bandwidth decreased to %11.49 and this layer which is added to increase the gain of the design also shifts the center frequency of the current design from 2410 MHz to 2610 MHz.

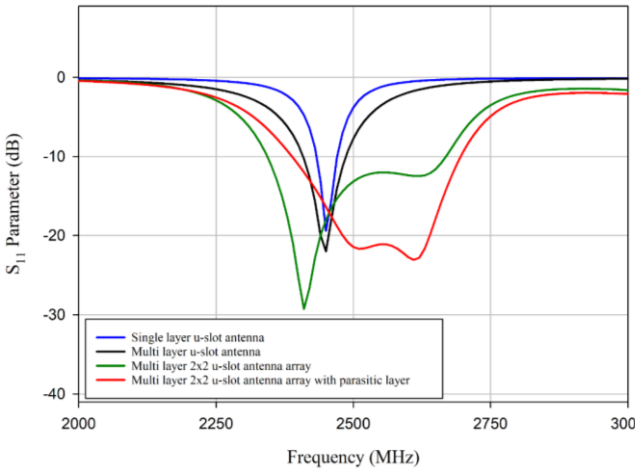

Figure 3. Simulated S_{11} plots of single layer U-slot antenna, multi-layer U-slot microstrip antenna and multi-layer 2x2 4-elements multi-layer antenna array.

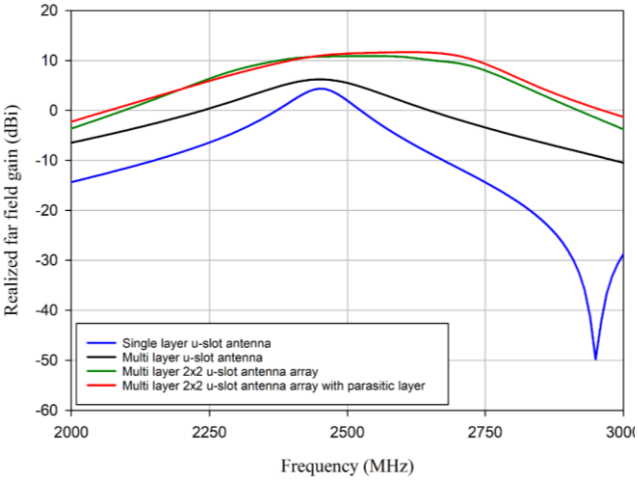

Figure 4. Realized far field gain (dBi) plots of single layer U-slot antenna, multi-layer U-slot microstrip antenna and multi-layer 2x2 4-elements multi-layer antenna array

Considering the realized far field gain (dBi) plots given in Figure 4, it can be observed that the gain of the single-layer U-slot microstrip antenna design with a center frequency of 2450 MHz increases from 4.37 dBi to 6.22 dBi with the multi-layer U-slot microstrip patch antenna design at the same operating frequency. Comparing the multi-layer single-element U-slot microstrip antenna design with the multi-layer 4-element U-slot microstrip patch antenna array in terms of gain, it is evident that the realized far field gain value rises from 6.22 dBi to 10.89 dBi. As the final stage of the design, the addition of a parasitic layer to the multi-layer 4-element U-slot microstrip antenna array further increases the gain value of the current design from 10.89 dBi to 12 dBi.

The 2D radiation pattern plot of each design stage is given in Figure 5.

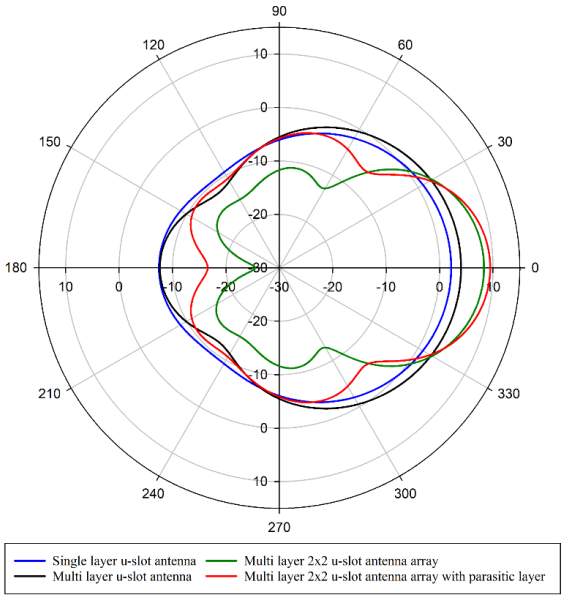

Figure 5. 2D Radiation pattern plots of single layer U-slot antenna, multi-layer U-slot microstrip antenna, multi-layer 2x2 antenna array, and multi-layer 2x2 antenna array with parasitic layer.

2.2 Antenna array design

The 2x2 U-slot microstrip antenna array design is carried out after the successful design and simulation of the single element U-slot microstrip antenna. The distance between the antenna array elements is considered to adjust within λ and $\lambda/2$. If the distance is set to greater than λ, grating lobes emerge on the radiation pattern. On the other hand, if the distance between the adjacent element is too lower than λ/2, it may cause undesired mutual coupling.

The proposed 2x2 4-elements antenna array design consisting of four layers is given in Figure 6. FR4 material with dielectric constant of 4.15 and the thickness of 1.59 mm is used as the dielectric substrate material for Layer 1, Layer 3 and Layer 4. PETG material with the dielectric constant of 2.62 and with the thickness of 3 mm is used as the dielectric substrate material for Layer 2. The three layers at the bottom are in contact with each other whereas the top layer is separated from the others by an air gap of 18.4 mm and is supported by rods made of PETG material. In this sandwich design, PETG material on Layer 2 is used to increase the bandwidth. An 8x8 elements of square microstrip patches printed on the FR4 material on Layer 4 are used to increase the gain of the array. Microstrip antennas are etched in the upper surface of Layer 3. The upper surface of this layer also contains the transmission lines. A detailed version of transmission line structure used in the design is given in Figure 6. These transmission lines consist of 50Ω and 100Ω lines and 70.71Ω quarter wavelength (λ/4) converters in order to eliminate the impedance mismatches. The quarter-wavelength transformers and transmission lines are initially designed by using the basic design formulas on a single-layer array and subsequently the whole array design is optimized by considering the multilayer structure. The initial design formulas for the antenna array implemented with quarter-wavelength transformers are provided in Equation (2).

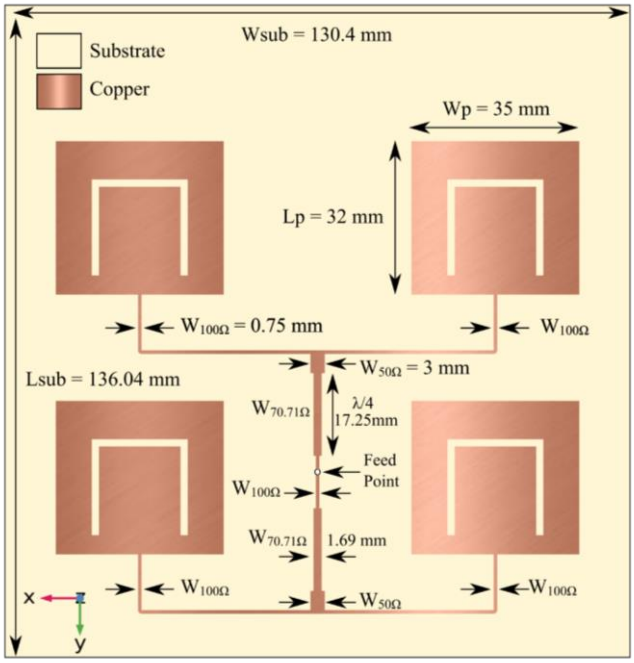

Figure 6. Microstrip antenna array transmission line structure.

$$Z_{in} = Z_1 \frac{Z_L + jZ_1 \tan \beta l}{Z_1 + jZ_L \tan \beta l} \quad (2.a)$$

$$Z_{in} = \frac{{Z_1}^2}{Z_L} \quad (2.b)$$

$$Z_1 = \sqrt{Z_0 Z_L} \quad (2.c)$$

In Equation (2.a), Z_{in} represents the input impedance observed at the matching section of the microstrip line when Z_1 denotes the characteristic impedance of the λ/4 long transmission line. Z_L represents target load impedance to be matched. At the design frequency impedance matching is achieved when the electrical length of the matching section is λ/4. In this equation $\beta l = (2\pi/\lambda)(\lambda/4) = \pi/2$. To simplify this equation we can divide the numerator and denominator by $\tan \beta l$ and take the limit as $\beta l \to \pi/2$ to get Equation (2.b). Considering the case of no reflection in the microstrip line ($\Gamma = 0$) the condition $Z_{in} = Z_0$ must be satisfied which yields the characteristic impedance Z_1 which is given in the Equation (2.c) [1]. The distance between each antenna element is adjusted to be 0.49 λ_0 horizontally and 0.33 λ_0 vertically to achieve maximum gain. Each antenna element is designed as a U-slot antenna and the whole

antenna array design operates at the center frequency of 2.61 GHz. The lower face of the FR4 material in Layer 1 is employed as a ground and the entire array is coaxially fed from a single point as shown in Figure 7.

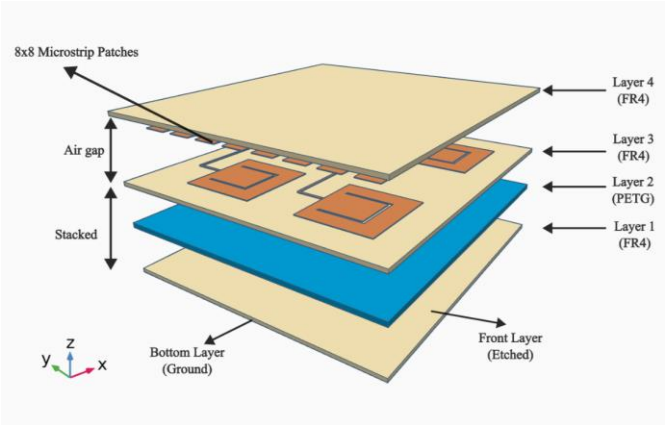

Figure 7. Exploded perspective view of 2x2 4-elements antenna array.

2.3 Parasitic array design and optimization

The parasitic layer in layer 4 is etched onto the bottom surface of an FR4 dielectric substrate, while the top surface of this dielectric substrate is completely etched. Square parasitic elements with a side of 10 mm (less than 0.1 λ_0) and periodicity of 5 mm (less than 0.1 λ_0) t are used while designing the parasitic layer. The parasitic square patch antenna array is initially designed to consist of 2x2 elements, then the design process is finalized to 8x8 elements in order to increase the gain of the antenna design. In this design process, from 2x2 elements to 8x8 elements, the distance of the parasitic layer to the antenna layer is optimized as h=5 mm, h=10 mm, h=15 mm and h=20 mm in order to obtain the highest gain. The flow diagram of the design process is given in Figure 8.

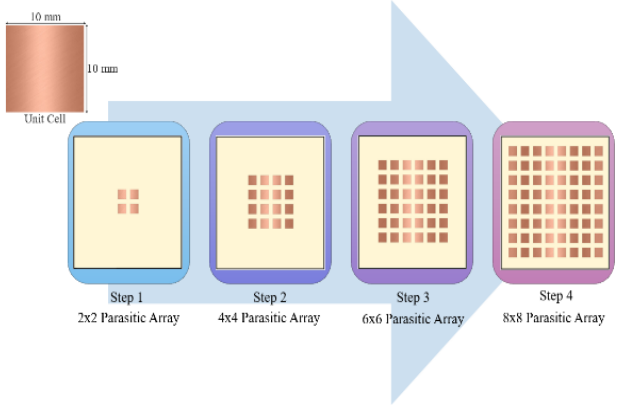

Figure 8. Parasitic layer evolution process.

The S_{11}, realized far field gain and 2D radiation pattern plots at the center frequency of each step are given in Figure 9.

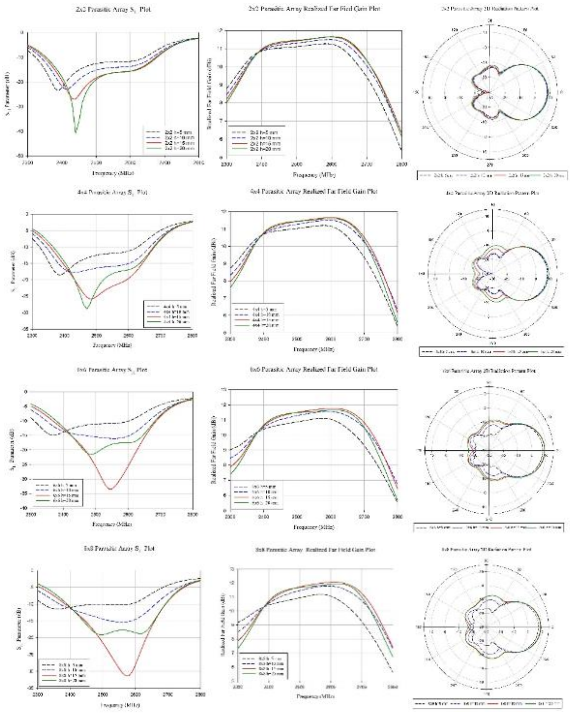

Figure 9. The S_{11}, realized far field gain and 2D radiation pattern plots at the center frequency of each design step.

When the graphs of each design stage given in Figure 9 are examined, it is observed that the center frequency and gain values change depending on the number of parasitic elements and the distance of the parasitic layer to the antenna layer. Considering each design step, it is seen that the highest gain is generally obtained when the distance from the parasitic layer to the antenna layer is h = 15 mm. In the final design, the 8x8 parasitic array design, this optimal height of 15 mm is optimized to obtain the highest gain again and the distance from the parasitic layer to the antenna layer is finally designed to be 18.4 mm. Figure 10 provides a detailed representation of the final parasitic layer design consisting of 8x8 square patch elements.

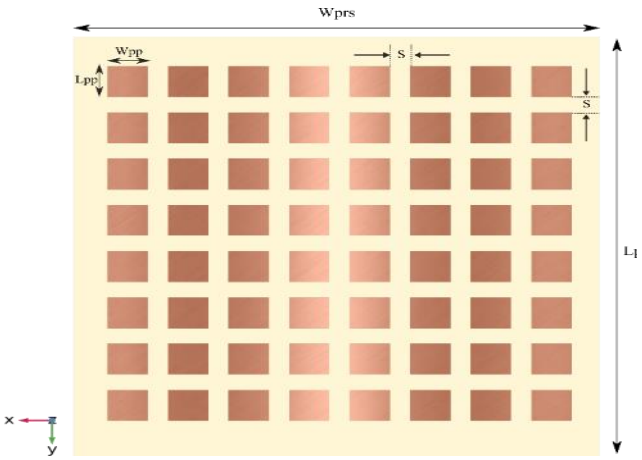

Figure 10. Top view of parasitic patch array. (W_{prs}=130.4 mm, L_{prs}= 136.04 mm, W_{pp}= 10 mm, L_{pp}=10 mm, S=5 mm).

3 Results and discussions

3.1 Simulated results

The design and simulation of the multilayer U-slot microstrip patch antenna array are performed by using Comsol 6.0 software with RF Module. Two illustrations of the antenna array structure are given in Figure 11.

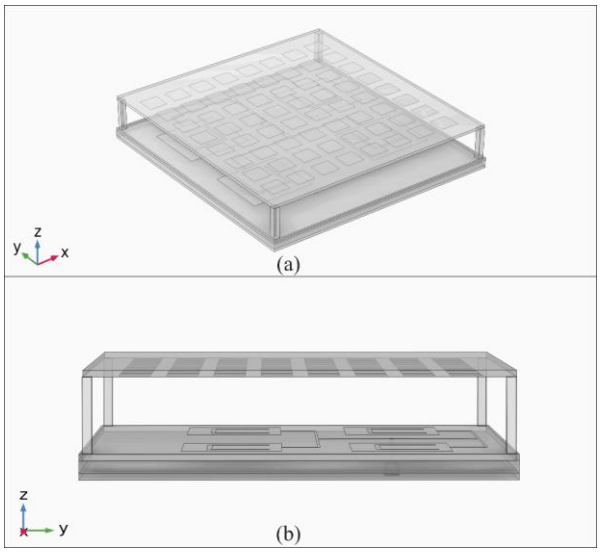

Figure 11. (a) Perspective and (b) side view of the proposed antenna array.

After the simulations, it is seen that the designed antenna has center frequency with the level of -22.75 dB at the 2610 MHz. Simulated reflection coefficient plot of the array is shown in Figure 12.

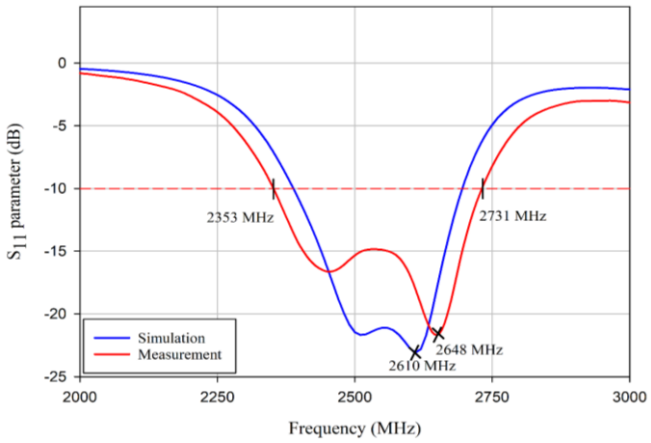

Figure 12. Simulated and measured S_{11} plot of the four elements array

The maximum gain of the 2x2 U-slot antenna array in the sandwich structure is measured as 12 dBi at the frequency of 2610 MHz. The designed antenna has a -10dB impedance bandwidth of %11.7 between 2390 MHz and 2690 MHz. The surface electric field distribution in the center frequency of the current design is given in Figure 13. The 2D and 3D radiation patterns of the designed antenna are given in Figure 15. The half power beamwidth is about 40° for both simulation and measured radiation patterns as shown in the same figure.

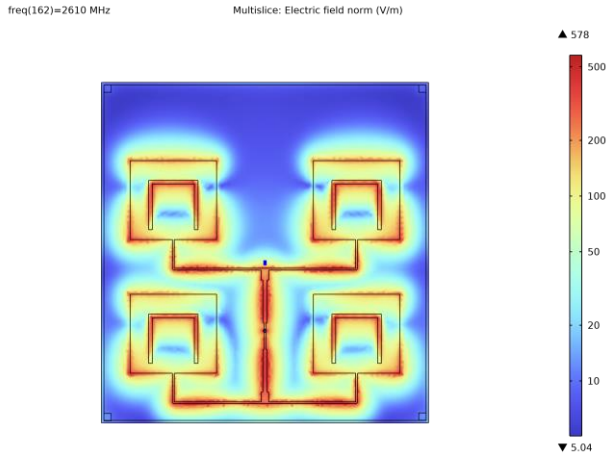

Figure 13. Surface electric field distrubition

3.2 Experimental results

A prototype of the proposed antenna design in this study is exhibited in Figure 14. In the manufactured antenna array, FR4 dielectric substrate material is used for the three layers. The dielectric substrate composed of PETG material in Layer 2 is fabricated using a 3D printer. FR4 material is used as the dielectric material to print the 2x2 U-slot antenna array and parasitic layer. The parasitic layer of the antenna array is isolated from Layer 3 by an air gap and supported with the help of rods made of PETG material.

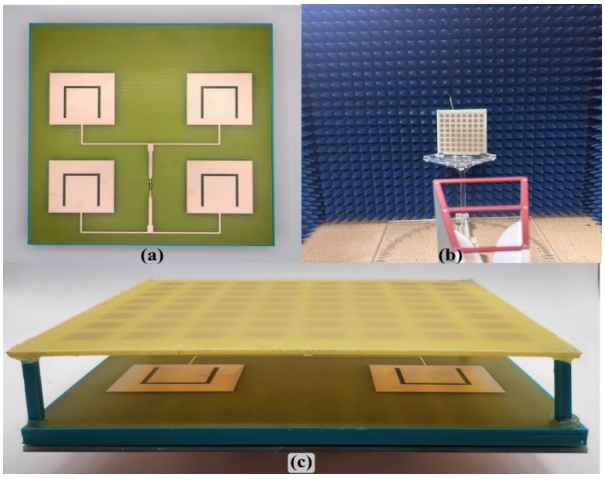

Figure 14. (a) Photographs of 2x2 antenna array layer, (b) radiation pattern measurement and (c) complete structure of proposed antenna

The reflection coefficient plot of the manufactured antenna array is measured by Rohde Schwarz ZNLE3 Vector Network Analyzer. The measured S_{11} plot compared with simulation results is given in Figure 12. When the plot of the measurement results given in Figure 12 is compared with that of the simulation results, it is observed that the measured

and simulated S_{11} plots are in a harmony. The -10 dB impedance bandwidth is obtained as %14.27 according to the measurement results. Since the achieved impedance bandwidth covers 2.4 GHz ISM band, the proposed antenna design is suitable for the ISM band applications. The comparison of the simulated and measured radiation patterns is given in Figure 15.

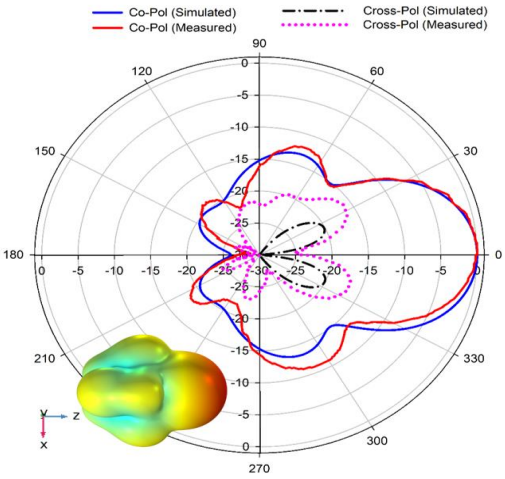

Figure 15. Simulated and measured co-polarization and cross-polarization radiation patterns of proposed antenna array in xz-plane

When the simulation and measurement results given in Figure 15 are evaluated, it is seen that results agree well. A maximum gain of 12 dBi is obtained with the simulated antenna array. Table II gives parameter comparisons of the proposed antenna with the multilayer antennas from the literature. The compared parameters in the table are electrical size, gain, impedance bandwidth, radiation efficiency and complexity.

It is clear from Table 2 that the designed and manufactured antenna in this study has the second smallest ground plane electrical size when it is compared with the given studies from the literature. Although the peak gain achieved in [33] is vaguely higher but it has bigger electrical ground plane size compared to our proposed antenna design. Similarly, while the antenna design in this paper exhibits lower gain compared to [34], it features a smaller ground plane electrical size and better radiation efficiency. The study reported in [35] has wider impedance bandwidth and smaller electrical size compared to proposed work but has lower gain. The antenna design having widest bandwidth in Table II is achieved in [36]. However, it has larger electrical ground plane size than that of the proposed antenna in this work also has the characteristics of lower antenna gain and radiation efficiency compared to this work. The antenna presented in [37] achieves a gain of 17.6 dBi which is better than that of our antenna design. Nevertheless, it has a narrower bandwidth and has larger ground plane dimensions in terms of the electrical sizes than the proposed design in this study also has a complex design.

4 Conclusion

In this study, a multi-layer, high-gain, 2x2 U-slot microstrip patch antenna array is designed, fabricated, and tested. The prototype measurements are in good agreement with the simulation results. Based on the measurement data, the proposed antenna has center frequency at 2.648 GHz. At 2.610 GHz, the array achieves a simulated maximum gain of 12 dBi and a radiation efficiency of 94.1%. The measured -10 dB impedance bandwidth is 14.27%, which covers the 2.4 GHz ISM band. This work demonstrates that the proposed antenna array offers high performance with a wide impedance bandwidth, making it suitable for various wireless communication applications. Potential improvements for future studies could involve altering the shape and number of the patch elements in the parasitic layer or adding extra layers to further optimize the antenna's performance. These modifications could result in an increased bandwidth, higher gain, and potentially enable multi-band operation, thereby broadening the antenna's potential applications.

Table 2. Performance comparison of the proposed antenna and the other antennas

Reference	Antenna Type	Size $\lambda_0 x \lambda_0 x \lambda_0$	Frequency (GHz)	Impedance Bandwidth	Gain (dBi)	Radiation Efficiency	Number of Layers	Complexity
33	2x2 Antenna Array	1.55 x1.55x0.11	5.85	%24.3 5.14 GHz- 6.56 GHz	12.5	NG	2	Moderate
34	2x2 Antenna Sub Array	1.4x1.4x0.161	12	%17.8	12.4	%85	3	Moderate
35	2x2 Antenna Array	0.98x0.98x0.047	2.45	%36.3	8.3 dBic	NG	2	Moderate
36	2x2 Antenna Array	1.374x1.374x0.078	5.35	%97.2 (2.75 GHz-7.95 GHz)	10.8	%88.5	2	Moderate
37	2x2 Antenna Array	6.68x6.68x0.837	20.02	%5.9 19.6 GHz-20.8 GHz	17.6	NG	3	Complex
This Work	2x2 Antenna Array	1.16x1.202x0.231	2.648	%14.27	12	%94.1	4	Moderate

* λ_0 is free space wavelength at the center frequency. **NG: Not Given.

Acknowledgement

This work is supported by the Scientific and Technological Research Council of Turkey (TUBITAK) under grant number 120E396

Conflict of interest

The authors declare that they have no conflict of interest.

Similarity Rate (iThenticate): 16 %

References

[1] D.M. Pozar, Microwave engineering. John Wiley & Sons, 2011.

[2] W. L. Stutzman and G. A. Thiele, Antenna theory and design. John Wiley & Sons, 2012.

[3] D. H. Schaubert, D. M. Pozar and A. Adrian. Effect of microstrip antenna substrate thickness and permittivity: comparison of theories with experiment, IEEE Transactions on Antennas and Propagation, 37, 6, 677-682, 1989. https://doi.org/10.1109/8.29353

[4] V.R. Gupta, N. Gupta, Two Compact Microstrip Patch Antennas for 2.4 GHz Band – A Comparison. Microwave Review, 12 (2), 29-31, 2006.

[5] H. R. Bae, S. O. So, C. S. Cho, J. W. Lee and J. Kim, A Crooked U-slot Dual-Band Antenna with Radial Stub Feeding. IEEE Antennas and Wireless Propagation Letters, 8, 1345-1348, 2009. https://doi.org/10.1109/LAWP.2009.2038937

[6] K. Wong, H. Chang, C. Wang and S. Wang, Very-Low-Profile Grounded Coplanar Waveguide-Fed Dual-Band WLAN Slot Antenna for On-Body Antenna Application. IEEE Antennas and Wireless Propagation Letters, 19 (1), 213-217, 2020, https://doi.org/10.1109/LAWP.2019.2958961

[7] J. J. Borchardt and T. C. Lapointe, U-slot Patch Antenna Principle and Design Methodology Using Characteristic Mode Analysis and Coupled Mode Theory. IEEE Access, 7, 109375-109385, 2019. https://doi.org/10.1109/ACCESS.2019.2933175

[8] C. Shekhar, An Optimized High Gain Microstrip Patch Array Antenna for Sensor Networks. International Conference on Communication, Networks and Computing, Springer, Singapore, 2018.

[9] C. Kumar, M. I. Pasha and D. Guha, Defected Ground Structure Integrated Microstrip Array Antenna for Improved Radiation Properties. IEEE Antennas and Wireless Propagation Letters, 16, 310-312, 2017. https://doi.org/10.1109/LAWP.2016.2574638

[10] B. Qian, X. Chen and A. A. Kishk, Decoupling of Microstrip Antennas with Defected Ground Structure Using the Common/Differential Mode Theory. IEEE Antennas and Wireless Propagation Letters, 20, 5, 828-832,2021. https://doi.org/10.1109/LAW P.2021.306 49 72

[11] F.Y. Zulkifli, E.T. Rahardjo and D. Hartanto, Radiation properties enhancement of triangular patch microstrip antenna array using hexagonal defected ground structure. Progress In Electromagnetics Research M, 5, 101-109,2008.https://doi.org/10.2528/PIERM0 81016 01

[12] M. Salehi, A. Tavakoli, A novel low mutual coupling microstrip antenna array design using defected ground structure, AEU-International Journal of Electronics and communications, 60 (10), 718-723, 2006. https://doi.org/10.1016/j.aeue.2005.12.009

[13] H. Alias, M. T. Ali, S. Subahir, N. Ya'acob and M. A. Sulaiman, Aperture coupled microstrip antenna array integrated with DGS and parasitic elements. 2013 IEEE Symposium on Wireless Technology & Applications (ISWTA),259-263,2013. https://doi.org/10.1109/ISWTA.2013.6688783

[14] R. -L. Xia, S. -W. Qu, S. Yang and Y. Chen, Wideband Wide-Scanning Phased Array with Connected Backed Cavities and Parasitic Striplines. IEEE Transactions on Antennas and Propagation, 66, 4, 1767-1775, 2018. https://doi.org/10.1109/TAP.2018.2803131

[15] C. Arora, S.S. Pattnaik and R.N. Baral, SRR Superstrate for Gain and Bandwidth Enhancement of Microstrip Patch Antenna Array. Progress In Electromagnetics Research B, 76, 73-85, 2017. https://doi.org/10.2528/PIERB17041405

[16] M. Asaadi and A. Sebak, Gain and Bandwidth Enhancement of 2 × 2 Square Dense Dielectric Patch Antenna Array Using a Holey Superstrate. IEEE Antennas and Wireless Propagation Letters, 16, 1808-1811,2017. https://doi.org/10.1109/LAWP.2017.2679698

[17] A.R. Vaidya, R.K. Gupta, S.K Mishra and J. Mukherjee, High-gain low side lobe level Fabry Perot cavity antenna with feed patch array. Progress In Electromagnetics Research C, 28, 223-238, 2012. https://doi.org/10.2528/PIERC12031503

[18] S. Dalvi, S. Jagtap, V. Yadav and R. K. Gupta, High gain wideband 2×2 microstrip array antenna using RIS and Fabry Perot Cavity resonator. 2016 International Conference on Microelectronics, Computing and Communications (MicroCom),1-6, 2016. https://doi.org/10.1109/MicroCom.2016.7522547

[19] S. Shingate, N. Shukla and N. R. Ingale, Bandwidth and Gain Enhancement of Microstrip Array Antenna using Stacked Layer of Parasitic Patches. 2018 3rd IEEE International Conference on Recent Trends in Electronics, Information & Communication Technology (RTEICT), 32-36, 2018. https:/doi.org/10.1109/RTEICT42901.2018.9012634

[20] A. M. Mehta, S. B. Deosarkar, and A. B. Nandgaonkar, Design and Development of CPW-fed Miniaturized MSA for Improved Gain, Bandwidth and Efficiency Using PRS. Progress in Electromagnetics Research C, 137,211–222,2023. https://doi.org/10.2528/PIERC23 0 71403

[21] M.A. Ramkumar, C. Sudhendra and K. Rao, A novel low RCS microstrip antenna array using thin and wideband radar absorbing structure based on embedded passives resistors. Progress In Electromagnetics

Research C, 68, 153-161, 2016. https:doi.org/10.2528/PIERC16080506

[22] B. Rana and S. K. Parui, Nonresonant Microstrip Patch-Fed Dielectric Resonator Antenna Array. IEEE Antennas and Wireless Propagation Letters, 14, 747-750, 2015. https://doi.org/10.1109/LAWP.2014.2379624

[23] J. -H. Ou, J. Huang, J. Liu, J. Tang and X. Y. Zhang, High-Gain Circular Patch Antenna and Array with Introduction of Multiple Shorting Pins. IEEE Transactions on Antennas and Propagation, 68, 9, 6506-6515, 2020. https://doi.org/10.1109/TAP.2020.2983793

[24] D. Helena, A. Ramos, T. Varum, and J. N Matos, Antenna design using modern additive manufacturing technology: A review. IEEE Access, 8, 177064-177083, 2020. https://doi.org/10.1109/ACCESS.2020.3027383

[25] S.S. Carvalho, J. R. Reis, A. Mateus and R. F. Caldeirinha, Exploring design approaches for 3D printed antennas. IEEE Access, 12, 10718-10735, 2024. https://doi.org/10.1109/ACCESS.2024.3354372

[26] J. Sun and F. Hu, Three-dimensional printing technologies for terahertz applications: a review. International Journal of RF and Microwave Computer-Aided Engineering, 30 (1), e21983, 2020. https://doi.org/10.1002/mmce.21983

[27] D. D. Patil, K. S. Subramanian and, N. C. Pradhan, 3-D-printed dual-band rectenna system for green IoT application. IEEE Transactions on Circuits and Systems II: Express Briefs, 70 (8), 2864-2868, 2023. https://doi.org/10.1109/TCSII.2023.3248171

[28] F. Pizarro, R. Salazar, E. Rajo-Iglesias, M. Rodriguez, S. Fingerhuth, and G.Hermosilla, Parametric study of 3D additive printing parameters using conductive filaments on microwave topologies. IEEE Access, 7, 106814-106823, 2019. https://doi.org/10.1109/ACCESS.2019.2932912

[29] M. A Belen, Stacked microstrip patch antenna design for ISM band applications with 3D-printing technology. Microwave and Optical Technology Letters, 61(3), 709-712, 2019. https://doi.org/10.1002/mop.31603

[30] G. Muntoni et al., A curved 3D-printed S-band patch antenna for plastic CubeSat. IEEE Open Journal of Antennas and Propagation, 3, 1351-1363, 2022. https://doi.org/10.1109/OJAP.2022.3222454

[31] M. F Farooqui, and A. Kishk, 3-D-printed tunable circularly polarized microstrip patch antenna. IEEE Antennas and Wireless Propagation Letters, 18 (7), 1429-1432, 2019. https://doi.org/10.1109/LAWP.2019.2919255

[32] G. G. B. Oner, S. Basbug and Y. Altuncu, Multi-Layer I-Slot Microstrip Antenna for Internet of Things Applications. 2023 14th International Conference on Electrical and Electronics Engineering (ELECO), Bursa, Turkiye, 2023, 1-4.https://doi.org/10.1109/ELECO60389.2023.10415969

[33] S. Jagtap, A. Chaudhari, N. Chaskar, S. Kharche and R. K. Gupta, A Wideband Microstrip Array Design Using RIS and PRS Layers. IEEE Antennas and Wireless Propagation Letters, 17 (3), 509-512, 2018. https://doi.org/10.1109/LAWP.2018.2799873

[34] F. Karami, P. Rezaei, A. Amn-e-Elahi, A. Abolfathi, and A. A. Kishk, Broadband and efficient patch array antenna fed by substrate integrated waveguide feed network for Ku-band satellite applications. International Journal of RF and Microwave Computer-Aided Engineering, 31 (9), 2021. https://doi.org/10.1002/mmce.22772

[35] P. Le Bihan et al., Dual-Polarized Aperture-Coupled Patch Antennas with Application to Retrodirective and Monopulse Arrays. IEEE Access, 8, 7549-7557, 2020. https://doi.org/10.1109/ACCESS.2019.2961601

[36] L. Gu, W. Yang, W. Feng, Q. Xue, Q. Meng and W. Che, Low-Profile Ultrawideband Circularly Polarized Metasurface Antenna Array, IEEE Antennas and Wireless Propagation Letters, 19 (10), 1714-1718, 2020. https://doi.org/10.1109/LAWP.2020.3014436

[37] X. Liu and Z. Yan, Broadband RCS reduction for both microstrip array and Fabry-Perot antenna based on the quasi- AMC superstrate. International Journal of RF and Microwave Computer-Aided Engineering, 31 (11), 2021. https://doi.org/10.1002/mmce.22838

[38] C. A. Balanis, Antenna Theory: Analysis and Design. John Wiley and Sons, 2016.